CHAPTER VII. ACCELERATING SCIENTIFIC HYPOTHESIS TESTING THROUGH MULTI-MODEL AI REASONING: CASE STUDIES IN OPTICS

DOI: 10.33407/lib.NAES.id/748238

Komarov Alexis[1][0009-0009-9544-1725]

[1] Institute of Physics of the National Academy of Sciences of Ukraine, Kyiv, Ukraine

alexis.komarov@iop.kiev.ua

Abstract. This study explores the transformative role of artificial intelligence (AI) tools in accelerating scientific hypothesis validation, focusing on the iterative use of reasoning and deep research large language models (LLMs). We classify LLMs into single-step, multi-step reasoning, and web-integrated deep research variants, demonstrating that ensembles of independent models enhance accuracy probabilistically from 8-27% for individual reasoning models to 48-62% for collective inference, when addressing complex physical queries. To illustrate the approach of collective AI inference, we examine case studies of diamond Bragg mirror reflectivity for keV-scale X-rays and metal vapor lasing for high-boiling-temperature metals. By iteratively prompting six LLMs with tailored queries and peer-reviewed data, we derive optimized theoretical results and experimental setups. The results underscore the ability of LLMs to accelerate scientific hypothesis testing, identify theoretical limits, and design experimental configurations while also highlighting the importance of verifying AI outputs, confronting AI with facts and follow-up questions, and accounting for AI model correlations. This framework pioneers a paradigm shift in interdisciplinary research, merging AI-driven reasoning with domain-specific expertise to resolve ambiguities in cutting-edge material science and photonics.

Keywords: Artificial intelligence, Reasoning models, Deep research, Diamond Bragg mirrors, Metal vapor lasers

Introduction. Artificial intelligence has already found multiple applications in business – such as chatbots, image and pattern recognition, personalized marketing, healthcare disease detection and drug discovery, language processing, fraud detection,

content creation, and energy management. Academic applications of AI are also emerging, particularly in data analysis (including pattern recognition, data mining, and statistical analysis), academic writing (such as style and grammar correction, translation, and plagiarism detection), and personalized tutoring. Typical accuracies of AI models in specialized applications are already high. For example, in natural language processing for translation, DeepL achieved 89% [1] accuracy in 2020, while Google Translate reached 86% in 2020 [1] and 80% [2] in 2022.

Scientific research is a relatively new field for artificial intelligence. Due to the inherent complexity of scientific research, both in breadth and depth, AI tools were not widely applied to it until around 2024. However, the emergence of large language models (LLMs) in 2022 has opened an entirely new class of AI applications in natural language processing. These applications include creating new scientific hypotheses, quickly testing hypotheses, identifying arguments and dependencies, stimulating creative thinking, comparing the outputs of various LLMs, synthesizing multiple arguments through reasoning, and selecting arguments that might explain observed physical processes. This work summarizes the current state of the most advanced LLMs, their potential applications in scientific hypothesis creation and testing, and proposes multi-model AI reasoning (MMAR) framework as a viable approach to improve the accuracy of human-guided scientific AI inference towards record 48-62%.

Literature Analysis and Problem Statement. The advancement of Large Language Models (LLMs) has catalyzed their adaptation for scientific reasoning, yielding distinct classes optimized for hypothesis testing and research workflows. These classes – single-step, reasoning, and deep research LLMs – differ fundamentally in their architectures, operational methodologies, and performance in scientific tasks. *Single-Step* Inference LLMs, such as GPT-3 [3], [4], GPT-3.5, GPT-4, and GPT-4o, represent the foundational paradigm of language models. These systems generate responses in a single pass, relying exclusively on static, pre-defined training datasets. While they excel at addressing straightforward queries with rapid responses and broad domain knowledge, their reliance on fixed datasets limits their utility in dynamic scientific contexts. Errors in complex reasoning tasks often arise due to the absence of

iterative validation, and their knowledge remains confined to information available up to their training cutoff dates. Despite these constraints, single-step LLMs remain widely used for basic question-answering and preliminary data interpretation. *Reasoning* LLMs enhance this framework by incorporating iterative, multi-step reasoning processes [5]. Unlike their single-step counterparts, these models – exemplified by OpenAI o1, o3, DeepSeek – employ techniques like chain-of-thought prompting [5], where each step of reasoning builds on prior outputs. This cumulative approach allows for incremental validation, significantly improving accuracy in tasks requiring abstraction, causal inference, or counterfactual analysis. However, the computational demand escalates with reasoning depth, and errors in early steps may propagate through subsequent stages [6]. Despite these trade-offs, reasoning LLMs demonstrate superior performance in hypothesis testing and experimental design compared to single-step systems. The most advanced class, *Deep Research* LLMs [7], integrates multi-step reasoning with real-time external data retrieval. These models, including OpenAI's o3-based DeepResearch, Perplexity's DeepSeek R1 Deep Research, and Grok 3 xAI's DeeperSearch, dynamically formulate search strategies by identifying key concepts within user queries. By accessing up-to-date scientific literature, clinical trials, or experimental datasets, they address the temporal limitations of static training data. This fusion of iterative reasoning and evidence-based validation achieves the highest accuracy in tasks such as literature synthesis, hypothesis generation, and experimental planning. For instance, Grok 3's multi-agent framework stress-tests hypotheses against conflicting data, while DeepSeek R1 optimizes search strategies for precision. However, their efficacy depends on the reliability of external sources and incurs higher computational costs and latency. Table 1 summarizes key characteristics of leading Deep Research LLMs available on the market as of March 2025 [9].

Table 1.

Accuracy of Deep Research LLMs with Reasoning and Web Search Functionality

Player	Model	Search features		Accuracy		Pricing
		Files	Web search	Correct	Incorrect	Monthly
				%	%	$
OpenAI	Deep Research	+	+	26.6%	73.4%	200
Perplexity	Deep Research	+	+	21.1%	78.9%	20
xAI	Grok 3 DeeperSearch	+	+	13.0%	87.0%	30
MiniMax	DeepSeek R1	+	+	9.4%	90.6%	0
DeepSeek	DeepSeek R1	+	-	8.9%	91.1%	20
Alibaba	QwQ 32B	+	+	8.2%	91.8%	0
Gemini	2.5 Pro Deep Research	-	+	5.3%	94.7%	0

Deep Research LLMs, leveraging dynamic data and multi-step workflows, attain the highest accuracy and adaptability to evolving scientific knowledge. Deep Research LLMs, such as Perplexity's Deep Research, exemplify the potential of democratizing the access to advanced inference, balancing high accuracy, computational efficiency, and cost. In the next section, we will demonstrate how combining Deep Research AI models can significantly enhance reasoning accuracy compared to individual models.

Research Methodology. The integration of multiple Deep Research Large Language Models (LLMs) represents a promising paradigm for improving accuracy in complex scientific reasoning tasks, particularly under conditions of uncertainty or incomplete data. This approach leverages probabilistic principles to mitigate individual model limitations, with implications for hypothesis validation, experimental design, and high-stakes decision-making. The ensemble efficacy arises from probability theory: For N independent models, each demonstrating a per-query accuracy of X_i, the probability that at least one model produces a correct answer is given by:

$$P_{\text{ensemble}} = 1 - \prod_{i=1}^{N} (1 - X_i)$$

This framework exponentially outperforms single-model accuracy when N > 1. However, there are critical caveats. First, models must exhibit independence to ensure errors remain uncorrelated (i.e., no shared training biases or data artifacts). Second, this

logic applies exclusively to binary outcomes, where responses are categorically correct or incorrect. A third requirement is static per-query accuracy, meaning model performance does not degrade with sequence length or task complexity.

To contextualize these principles, consider the Humanity's Last Exam benchmark – a simulated high-difficulty scientific reasoning test [8]. Empirical results demonstrate that an ensemble of the top six models (with accuracies as listed in Table 1) achieves a combined accuracy of 62%, while excluding computationally expensive and costly OpenAI Deep Research model reduces this to 48%. Individual models exhibit modest accuracy (5.3 – 26.6%), but strategic ensemble combinations yield disproportionate gains. Notably, the 62% ensemble accuracy surpasses the best single-model performance by 35%, aligning with theoretical predictions.

Table 2.

Theoretical Combined Accuracy of Top 6 Deep Research LLMs with Reasoning and Web Search Functionality

Player	Model	Search features		Accuracy		Pricing
		Files	Web search	Correct	Incorrect	Monthly
				%	*%*	*$*
Top 6 models		+	+	61.8%	38.2%	270
Top 6 models excl. OpenAI		+	+	48.0%	52.0%	70

Implementation Framework

The initial step involves the identification and clear delineation of the research *objective*. This is achieved through an extensive review of the existing literature, ensuring that the objective is both well-founded and contextually relevant. A panel of AI tools is then employed to determine the key *drivers* that are critical to achieving or maximizing the stated objective. These drivers represent the primary variables or conditions that may influence the outcome of the hypothesis validation process. The outputs from the various AI tools are synthesized to compile an *exhaustive list* of drivers. This comprehensive list forms the basis for subsequent analytical steps and ensures that all relevant factors are considered. Utilizing the complete list of drivers, a targeted prompt is developed with the explicit goal of optimizing the pathway to the stated objective. The prompt is designed to guide the AI models toward generating outputs that directly address the interplay of the

identified drivers. The responses produced by the AI models are systematically analyzed to identify convergence and divergence in the generated solutions. When outputs converge with minimal discrepancies, the result is interpreted as a viable solution, warranting further validation by a human expert. Conversely, if discrepancies or gaps are observed – where the AI tools provide conflicting responses – these gaps are documented for further analysis. In cases where discrepancies are present, the framework prescribes an iterative approach. The prompt is modified to explicitly incorporate the identified gaps, and the refined prompt to maximize the objective taking into account the gaps is reintroduced into the AI analysis cycle. This process is repeated. If subsequent iterations yield convergent responses or successfully bridge the gaps, the solution is considered validated and may serve as a working hypothesis to be presented to a human expert. If significant discrepancies persist despite iterative refinements, it may be concluded that a solution is not attainable with the current set of AI tools. Fig. 1 shows the approach.

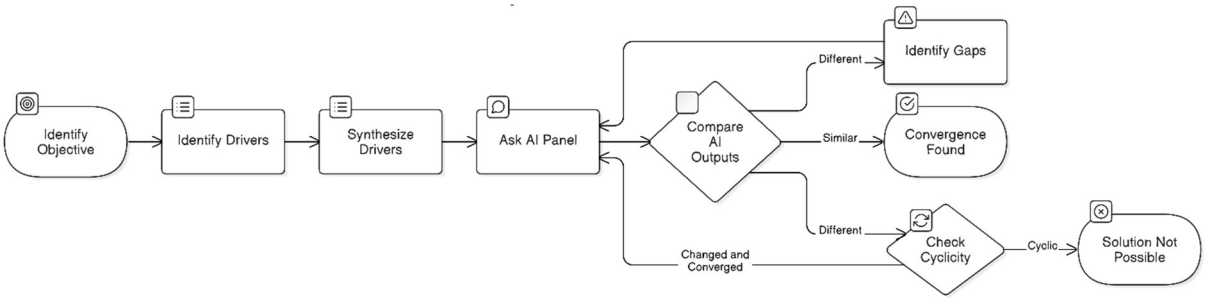

Fig. 1. AI-Assisted Process for Validating Scientific Hypotheses

Case 1: Single Crystal Diamond Bragg Mirror Reflectivity for keV X-rays

The development of high-reflectivity X-ray optics faces significant challenges due to the stringent material requirements for manipulating high-energy photons. While Mo/Si, Mo/B4C, Ru/B4C, W/C, W/Be, Si/C mirrors achieve 70–90% reflectivity [11], [12], [13] at grazing angles of incidence in the extreme ultraviolet (EUV) range (e.g., 13 nm lithography systems) and X-ray range, dielectric mirrors in the near-infrared (NIR) exhibit near-perfect reflectivity (99.9998%) with transmission, scattering, and absorption losses as low as 1.6 ppm [14], [15]. Recent advances in single-crystal diamond Bragg mirrors have demonstrated exceptional reflectivity (>99%) for keV-scale X-rays at near-normal incidence [16], enabling novel applications in X-ray free-electron laser oscillators

(XFELOs) and coherent X-ray pulse stacking. However, the theoretical upper bounds of diamond reflectivity remain unresolved due to complexities in the dynamic theory of Bragg diffraction. To address this, a multi-model artificial intelligence (AI) framework was deployed to systematically evaluate hypotheses governing diamond mirror performance.

A panel of AI Deep Research models – Perplexity Deep Research, MiniMax DeepSeek-R1, Grok 3 DeeperSearch, and OpenAI o3-mini – was leveraged to analyze critical variables influencing single crystal diamond Bragg mirror performance. Specialized prompts were iteratively refined to query *dominant drivers* of reflectivity, including material properties (high Debye temperature, low atomic number of diamond), structural perfection (dislocation density), X-ray energy (higher energy implies lower photoelectric absorption and Compton scattering), crystal geometry (sufficient thickness to reflect more than 99% of X-rays, Bragg reflection choice), operating conditions (temperature minimizing lattice vibrations, narrow X-ray bandwidth to fit with the Bragg reflection), isotopic purity (^{12}C single crystal diamond has slightly higher Debye temperature and lower lattice vibrations).

Having identified all possible drivers of diamond mirror reflectivity, research strategy was focused at *estimating theoretical limits* under idealized conditions (zero dislocation density, cryogenic operating temperatures, isotopic ^{12}C purity, sufficient thickness, right choice of the Bragg reflection, narrow X-ray bandwidth to fit the Bragg reflection). This translated into estimating minimum extinction length and highest absorption length to maximize reflectivity according to a classic formula:

$$\langle R_H \rangle \approx 1 - \frac{3\pi}{4} \frac{L_{\text{ext}}}{L_{\text{abs}}}$$

A prompt "What are the absorption and extinction lengths (mm) of ideal ^{12}C diamond at 77K cryogenic temperature with zero dislocation density for 23.765 keV, 13.903 keV, 31 keV, 35 keV, 44 keV X-rays?" was created. Inputs included peer-reviewed studies of Shvyd'ko et al., 2011 [16], computational datasets from the NIST X-ray mass attenuation database, and dynamical diffraction theory. Model responses were cross validated according to the methodology (Fig. 1). According to the models, the maximum attainable

reflectivity of a diamond X-ray Bragg mirror in backscattering (normal-incidence Bragg geometry) is achieved at 13.903 keV and is estimated at 99.97% (Grok-3 Think). This compares to 99.10% reflectivity actually measured at 13.903 keV, as experimentally demonstrated in [16]. Such a high reflectivity of 99.97% could theoretically enable multi-pass resonators sustaining high efficiency for more than 1,000 passes.

Case 2: Metal Vapor Lasers

Metal vapor lasers were among the first types of lasers discovered in the 1950s and 1960s, alongside dye and semiconductor lasers. Although other types of lasers – such as CO_2 lasers, fiber lasers, and diode-pumped solid-state lasers have since captured a larger share of the market, metal vapor lasers remain highly valued. They offer a wide range of over 480 different wavelengths, spanning from 224 nm to 6,457 nm, along with pulse durations in the nanosecond range, very narrow spectral lines for precise wavelength control, and high pulse repetition rates of several kilohertz. Laser emission has been observed in a total of 32 metals and 3 nonmetals, including Ag, Al, As, Au, Ba, Be, Bi, Ca, Cd, Cs, Cu, Dy, Eu, Fe, Ga, Hg, I, K, Mg, Mn, Na, Pb, Rb, Se, Sm, Sn, Sr, Ta, Te, Ti, Tl, Tm, V, Yb, and Zn [17].

Table 3.

Sample Characteristics of Metal Vapor Lasers

Metal	Melting point	Boiling Point	Temp (theory)	Temp (experiments)	Vapor production	Pumping	Efficiency	Peak Power	Avg Power
	K	*K*	*K*	*K*			*%*	*W*	*W*
Ta	3,290	5,731	3,152	...	Nd:YAG laser ablation	KrF excimer laser, 10 mJ	0.010%	48	0.16
V	2,183	3,680	2,024	...	Nd:YAG laser ablation	XeCl excimer laser, 25 mJ	0.001%	7	0.35
Ti	1,941	3,560	1,958	...	Excimer laser ablation	N2 laser, 0.2-5 mJ, Tunable dye laser,	...	...	...
Fe	1,811	3,135	1,724	973	Iron vaporization, FeBr2 vaporization, laser ablation	KrF excimer laser, 34 mJ	0.007%	180	...
Au	1,337	3,129	1,721	383 - 1,923	Gold vaporization, HAuCl4 vaporization	Discharge	0.230%	12,000	10
Sn	505	2,875	1,581	1,673	Tin vaporization	Discharge	0.002% - 0.200%	~10,000	10
Dy	1,685	2,840	1,562	1,723	Dysprosium vaporization	Discharge	0.084%	333	0.08
Cu	1,358	2,835	1,559	673 - 1773	Copper vaporization, CuBr vaporization	Discharge	2.900%	305,000	312
Be	1,560	2,744	1,510	773 - 2,273	Beryllium vaporization, BeCl2 vaporization	Discharge	...	1-10	<1
Al	933	2,740	1,507	473 - 1,773	Aluminum vaporization, AlCl3 / AlBr3 vaporization	Discharge	...	...	...
Ga	303	2,676	1,472	773 - 1,673	Nd:YAG laser ablation, GaCl3 / GaBr3 vaporization	TEM00 diodes at ~400 nm	...	...	<0.06
Ag	1,235	2,435	1,340	873 - 1,425	Discharge, AgBr vaporization	Discharge	0.004%	600	0.14
Mn	1,519	2,334	1,284	920 - 1,450	Manganese vaporization, MnCl2 vaporization	Discharge	0.200%	24,000	7.4
Tm	1,873	2,223	1,223	1,420 - 1,440	Thulium vaporization	Discharge	0.130%	20,800	0.5
Ba	1,000	2,118	1,165	1,120	Barium vaporization	Discharge	0.720%	100,000	12.5
Sm	1,345	2,067	1,137	1,873	Samarium evaporation, SmCl3 evaporation (n/a)	Discharge, Tunable dye laser	...	...	...
Pb	601	2,022	1,112	1,010 - 1,210	Lead evaporation	Discharge	0.090%	34,000	0.9
Eu	1,099	1,802	991		Europium evaporation	Discharge	0.300%	...	2.5
Sr	1,042	1,657	911	1,073	Strontium vaporization, SrBr2 vaporization	Discharge	7%?	48,333	29.0
Cd	594	1,040	572	523	Cadmium evaporation	Discharge	0.400%	...	0.194
K	336	1,032	568	380	Potassium evaporation	Diodes	41.140%	230,000	4,200
Rb	312	961	529	386	Rubidium evaporation	Diodes	33.000%	...	34,000
Cs	302	944	520	393	Cesium evaporation	Diodes	33.000%	...	2,000
Hg	234	630	347	349	Mercury vaporization	Discharge, Flashlamp	0.016%	5,520	0.24
I	387	457	251	313	Iodine evaporation	Flashlamp	2.000%	3,000,000,000,000	0.67

However, the energy conversion efficiencies of metal vapor lasers are relatively low, ranging from 0.01% to 2.9%, except in the case of alkali vapor lasers, for which efficiencies of 33-41% have been demonstrated [18], [19]. In addition, due to constraints of optical

materials (mirrors, lenses, Brewster plates), lasing in some refractory metals with high evaporation temperatures (Mo, W, Th, U and other) have not yet been demonstrated. In this example, AI could be used to elucidate if these specific metals could exhibit vapor lasing at specific conditions and vapor production setups. The query starts with the definition of a clear objective: "How could metal vapor lasing be demonstrated in refractory metals (Mo, W, Th, U…)? What are the key parameters controlling metal vapor lasing in these metals?". Synthesis of AI model outputs has allowed to identify the main demonstration methods for metal vapor generation: pulsed pico- and femtosecond laser ablation, electron beam heating, chemical vapor transport (metal halides, metal fluorides), and ion beam sputtering. Key parameters governing metal vapor lasing turned out to be laser transitions, vapor density (10^{14}+ / cm^3), vapor pressure related to vapor density, vapor temperature, buffer gas composition (He / Ne / Ar), pump wavelength matching atomic absorption lines, pump source (tuneable dye lasers, laser diodes, other lasers, electric discharge), upper state lifetime (10^{-9}+ s). Afterwards, the objective maximization question is asked: "Which parameter values (methods of metal vapor generation, laser transitions, vapor density, vapor pressure, vapor temperature, buffer gas composition, pump wavelength matching, pump source, upper state lifetime) could enable experimental demonstration of Mo, W, Th, and U metal vapor lasers taking into account temperature constraints (optic elements), and what could be the experimental setups?". A panel of AI tools gives multiple answers, which are then carefully reviewed and reconciled. Optimal experimental configuration is then selected among the options provided.

Conclusions. The findings presented here illustrate the potential of a multi-model AI reasoning framework to accelerate scientific hypothesis testing and refine experimental designs in advanced optics. By combining a panel of deep research large language models (LLMs), we demonstrated how ensembles of AI systems can surpass individual model performance in tackling complex physical inquiries, achieving accuracy gains from 8-27% to approximately 48–62%. These improvements were confirmed through iterative prompting, data cross-validation, and the strategic integration of domain knowledge.

In the case studies of diamond Bragg mirrors for keV X-rays and high-boiling-temperature metal vapor lasers, multi-model inference facilitated the identification of

crucial material parameters, boundary conditions, and theoretical limits, while also guiding the design of experimental setups. Specifically, for diamond mirrors, the combined AI approach uncovered optimal reflectivities and crystal purity conditions, suggesting that near-perfect reflectivity – while attainable in principle – remains constrained by practical material imperfections and absorption limits. Likewise, in metal vapor lasers, multi-model reasoning revealed key drivers of lasing thresholds and design requirements for sustaining high-temperature vapor states.

These results underscore both the promise and the challenges of AI-driven scientific research. On one hand, iterative AI–human interactions can highlight new opportunities for hypothesis generation and testing, boosting efficiency in fields where physical experiments are time-consuming and resource-intensive. On the other hand, thorough verification of AI outputs remains essential. Model correlations, shared biases, and potential "hallucinations" necessitate domain-expert oversight and well-designed prompts that confront AI with updated facts, boundary checks, and iterative follow-up questions.

Overall, this study indicates that AI systems can serve as potent collaborators in science, guiding researchers toward higher-accuracy theoretical predictions and experimental designs in less time. Future work should further examine the independence of different AI models, develop more robust strategies to mitigate correlated errors, and integrate domain-specific constraints that help sustain validity when extrapolating beyond existing knowledge. By merging multi-model AI reasoning with human expertise, researchers can unlock more rapid, rigorous, and creative solutions in emerging frontiers of optics, materials science, and beyond.

References

1. Hidalgo-Ternero, C. M. (2020). Google Translate vs. DeepL: analysing neural machine translation performance under the challenge of phraseological variation.

2. Saputra, A. (2022, June). The analysis of Google translate accuracy in translating procedural and narrative text. In Journal of English Education Forum (JEEF) (Vol. 2, No. 1, pp. 7-11).

3. Brown, T., Mann, B., Ryder, N., Subbiah, M., Kaplan, J. D., Dhariwal, P., ... & Amodei, D. (2020). Language models are few-shot learners. Advances in neural information processing systems, 33, 1877-1901.

4. Zhao, W. X., Zhou, K., Li, J., Tang, T., Wang, X., Hou, Y., ... & Wen, J. R. (2023). A survey of large language models. arXiv preprint arXiv:2303.18223, 1(2).

5. Wei, J., Wang, X., Schuurmans, D., Bosma, M., Xia, F., Chi, E., ... & Zhou, D. (2022). Chain-of-thought prompting elicits reasoning in large language models. Advances in neural information processing systems, 35, 24824-24837.

6. Pfister, R., & Jud, H. (2025). Understanding and Benchmarking Artificial Intelligence: OpenAI's o3 Is Not AGI. *arXiv preprint arXiv:2501.07458*.

7. Wu, J., Zhu, J., & Liu, Y. (2025). Agentic Reasoning: Reasoning LLMs with Tools for the Deep Research. arXiv preprint arXiv:2502.04644.

8. Phan, L., Gatti, A., Han, Z., Li, N., Hu, J., Zhang, H., ... & Verbeken, B. (2025). Humanity's Last Exam. *arXiv preprint arXiv:2501.14249*.

9. Artificial Analysis (2025, March), Comparison of Models: Intelligence, Performance, and Price Analysis

10. Perplexity AI (2025, February). Introducing Perplexity Deep Research

11. https://henke.lbl.gov/optical_constants/multi2.html

12. Huang, Q., Liu, Y., Yang, Y., Qi, R., Feng, Y., Kozhevnikov, I. V., ... & Wang, Z. (2018). Nitridated Ru/B4C multilayer mirrors with improved interface structure, zero stress, and enhanced hard X-ray reflectance. Optics Express, 26(17), 21803-21812.

13. Akhsakhalyan, A. D., Kluenkov, E. B., Lopatin, A. Y., Luchin, V. I., Nechay, A. N., Pestov, A. E., ... & Shcherbakov, A. V. (2017). Current status and development prospects for multilayer X-ray optics at the Institute for Physics of Microstructures, Russian Academy of Sciences. Journal of Surface Investigation: X-ray, Synchrotron and Neutron Techniques, 11, 1-19.

14. Rempe, G., Thompson, R. J., Kimble, H. J., & Lalezari, R. (1992). Measurement of ultralow losses in an optical interferometer. Optics letters, 17(5), 363-365.

15. Truong, G. W., Winkler, G., Zederbauer, T., Bachmann, D., Heu, P., Follman, D., ... & Cole, G. D. (2019). Near-infrared scanning cavity ringdown for optical loss characterization of supermirrors. Optics Express, 27(14), 19141-19149.

16. Shvyd'ko, Y., Stoupin, S., Blank, V., & Terentyev, S. (2011). Near-100% Bragg reflectivity of X-rays. Nature Photonics, 5(9), 539-542.

17. Little, C. E. (1999). Metal vapour lasers: Physics, engineering and applications (p. 646).

18. Zweiback, J., Hager, G., & Krupke, W. F. (2009). High efficiency hydrocarbon-free resonance transition potassium laser. *Optics Communications*, *282*(9), 1871-1873.

19. Biswal, R., Mishra, G. K., Agrawal, S. K., Dixit, S. K., & Nakhe, S. V. (2019). Studies on the design and parametric effects of a diode pump alkali (rubidium) laser. *Pramana*, *93*, 1-9.

* * *